THE CHALLENGES OF USING DOUBLE TARGETS AS A NOVEL CONTRAST-ENHANCEMENT METHOD FOR LASER-DRIVEN ACCELERATION

Laurențiu DINCĂ[1,2], Cosmin JALBĂ[1,2], Bogdan DIACONESCU[3], Mihail CERNĂIANU[4], Petru GHENUCHE[3], Bogdana MITU[5], Theodor ASAVEI[6], Florin ROTARU[7]

Laser-driven proton acceleration by Target Normal Sheath Acceleration (TNSA) is often performed using thick foil targets. For an efficient acceleration process, the High-Power Laser (HPL) incident on the foil requires sufficient contrast. To meet this requirement, we investigated the use of targets with a spaced bilayer structure consisting of an ultra-thin solid film (nm) in the front, a void of tens of μm thickness and a foil in the rear, focusing the laser pulse on the foil front surface. Diamond-Like Carbon (DLC) thin films free-standing on Cu substrates were fabricated, characterized, incorporated into carbon-Al double targets, and tested at pulse intensities of ~10^{20} W/cm^2.

Keywords: diamond-like carbon; free-standing film; high-power laser; target normal sheath acceleration.

1. Introduction

In the last decades, the research on laser-driven ion/electron acceleration has experienced enormous progress since the implementation of chirped pulse amplification and diffraction grating compression in the HPL research field. These two techniques have allowed the development of laser systems with increasing

[1] PhD student, SDIALA, National University of Science and Technology POLITEHNICA BUCHAREST (UNSTPB), Bucharest, Romania
[2] Doctoral research assistant, ELI-NP, HORIA HULUBEI National Institute for R&D in Physics and Nuclear Engineering (IFIN-HH), Măgurele, Romania,
e-mail: laurentiu.dinca@eli-np.ro, cosmin.jalba@eli-np.ro
[3] Senior research scientist 2nd degree, ELI-NP, HORIA HULUBEI National Institute for R&D in Physics and Nuclear Engineering (IFIN-HH), Măgurele, Romania,
e-mail: bogdan.diaconescu@eli-np.ro
[4] Engineer, ELI-NP, HORIA HULUBEI National Institute for R&D in Physics and Nuclear Engineering (IFIN-HH), Măgurele, Romania, e-mail: mihail.cernaianu@eli-np.ro
[5] Senior research scientist 1st degree, National Institute for R&D in Laser, Plasma and Radiation Physics (INFLPR), Măgurele, Romania, e-mail: mitu.bogdana@inflpr.ro
[6] Junior research scientist 3rd degree, ELI-NP, HORIA HULUBEI National Institute for R&D in Physics and Nuclear Engineering (IFIN-HH), Măgurele, Romania
[7] Research scientist 3rd degree, DFN, TANDEM, HORIA HULUBEI National Institute for R&D in Physics and Nuclear Engineering (IFIN-HH), Măgurele, Romania

pulse intensities over time [1], reaching in recent years $10^{19}\div10^{21}$ W/cm^2 in most experimental setups [2]. Several types of acceleration mechanisms are mentioned in the scientific literature on HPL-target interaction, and the dominant mechanism involved in a particular experiment depends on the characteristics of target and incident laser pulse. The TNSA is the first employed mechanism and is dominant when target films (with typical thickness in the μm range) are shot with HPL pulses of intensity $I>10^{18}$ W/cm^2 [3]. The TNSA is based on the charge separation between positive ions and electrons caused by the high electromagnetic field of the focused HPL beam. In the target film, the atoms are ionized, the electrons are spatially separated from ions and quickly accelerated in the direction of laser propagation due to their high mobility. This dynamics promotes the ion acceleration from the contaminant layer on the film rear side under the electrostatic field of the electron sheath in motion [4].

In the TNSA regime, the kinetic energy of accelerated ions is proportional to the square root of incident HPL intensity [5]. A proper contrast ratio (the ratio of the main pulse to prepulse intensity) is required for an efficient interaction of the main laser pulse with the target front surface. At intensities higher than 10^{20} W/cm^2, a low contrast pulse can lead to uncontrolled phenomena such as target destruction before the main pulse arrives [3], while a high contrast prevents them. The proper control of the duration and intensity of HPL prepulse contributes to get a preplasma enriched with hot electrons. During main pulse interaction, this leads to an increased charge separation whose strong electric field improves the ion cut-off kinetic energy [6, 7]. The contrast enhancement is obtained after the prepulse cleans of HPL pulse and is currently performed using plasma mirrors located in the pulse path in front of target, such as single/double plasma mirrors, supplementary providing direct protection against back reflection [8, 9]. This work [10, 11] investigates a contrast enhancement mechanism not requiring an external plasma mirror, but instead a target with a special double layer structure (double target). The underlying phenomena consists in the turning the first ultrathin film (nm thickness) into plasma by absorbing a large part of incident prepulse energy, afterwards the plasma becomes transparent to the main pulse. As a result the main pulse, enhanced in contrast, will hit the main target (second foil) tens of μm away from the sacrificial target (Fig. 1).

Within the first phase of the 1 PW commissioning experiments, we have fabricated double targets which were used to elucidate some aspects of the interaction between low contrast laser pulses and solid targets without using any plasma mirror. Despite of some unknowns regarding laser parameters existed in the ramp-up phase of experiments, the back reflection determinations could help to a qualitative description of laser pulse from the point of view of prepulse shape or contrast.

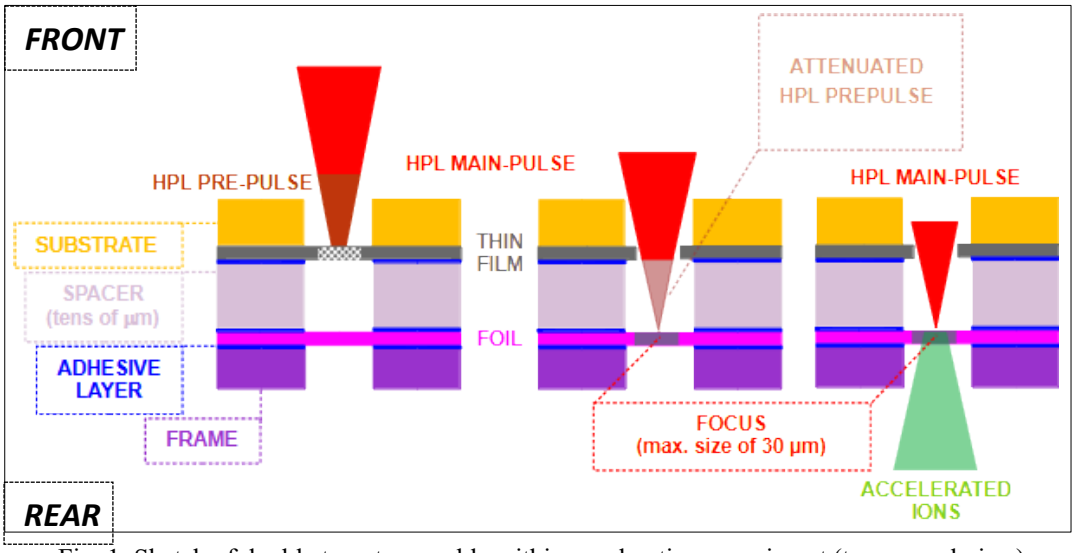

Fig. 1. Sketch of double target ensemble within acceleration experiment (transversal view)

We have fabricated double targets using Al target foils of 15 µm thickness and free-standing, nanometer thick DLC as ultra-thin solid films supported on patterned Cu substrates. The back reflection measurements were performed on these target ensembles within preliminary tests in 1 PW E5 experimental area [12] of ELI-NP, under HPL pulses to indirectly test the contrast enhancement efficiency. This assumes that the laser pulse should have a lower back reflection on the single Al-foil target than on the double target after properly functioning as described above.

2. Fabrication of DLC-Al double targets

The DLC films were grown on bulk Cu substrates by PECVD using CH_4/H_2 gaseous mixture with high H_2 content at total pressure of ~10^{-3} mbar, with plasma generated in radiofrequency (RF) electric field of 13.56 MHz and 100 W power.

After DLC deposition, the free-standing films was achieved by patterned chemical back-etching in a 10-holes map, which consisted of the following steps:

- spraying of positive photoresist and thermal curing (90°C, 30 min after an increasing ramp) for each side of DLC/Cu sample;
- masking of DLC/Cu sample to subsequent UV exposure (UV mask);
- UV exposure in 4 positions, each for 1 min (total of 4 min);
- unmasking;
- developing for ~3 min in sol. NaOH 10 g/L (the removal of exposed photoresist);

- etching of Cu substrate for ~40 min in sol. $FeCl_3$ (conc. 40%) under mechanical agitation, guided by the photoresist film pattern previously transferred during the developing;
- careful rinsing in acetone (the removal of unexposed photoresist).

The target holder system includes a carrousel for the Al frames, each of which can sustain one usable target by bonding the surfaces. In order to mount the double targets on the frames (Fig. 2) and to hold these on carrousel, the following steps were performed:

- cutting four fragments from one corroded DLC/Cu sample having thin DLC film;
- cleaning Al frame and fixing Al foil (target itself) on it by gluing with Canada balsam (adhesive layer formation between foil and frame surfaces);
- fixing by gluing with Canada balsam of one Al foil or many Al foils (stack) on target itself (on the area common to Al frame) to form a spacer between target itself and fragment of corroded DLC/Cu sample subsequently fixed on spacer;
- fixing DLC/Cu fragment on spacer with the substrate and frame holes and the Al foil in alignment, using PMMA acetonic solution which sustains the fragment more weightier than foil;
- mounting and optical pre-alignment of these target ensembles on the carrousel of the target holder system which gives a stellar configuration of the lot of target ensembles used.

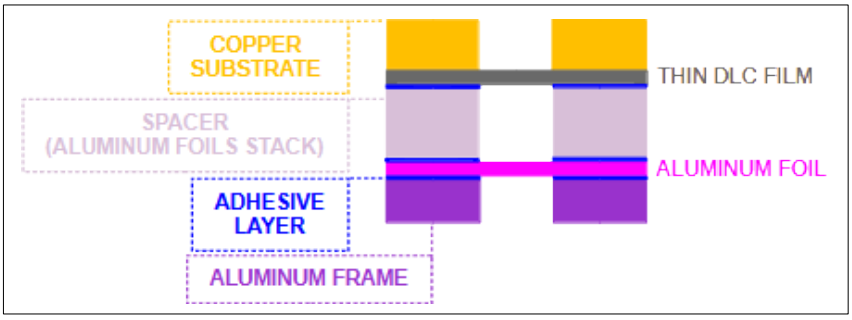

Fig. 2. Sketch of double target – frame ensemble (transversal view)

3. Characterization of free-standing DLC films

The statistical distribution of the average size of the holes obtained using the previously described procedure is illustrated (including the minimum, maximum, mean, standard deviation STD) in the histogram of Fig. 3. The mean size of all achieved free-standing zones was 1035.43 μm, similar with the diameter of UV mask holes (1 mm ± 0.1 mm), having the STD of 293.64 μm and the values ranging from 471.63 μm to 1988.83 μm. The large aperture dimension variation

comes from overexposure during masking and long and varying etching times of the copper substrate.

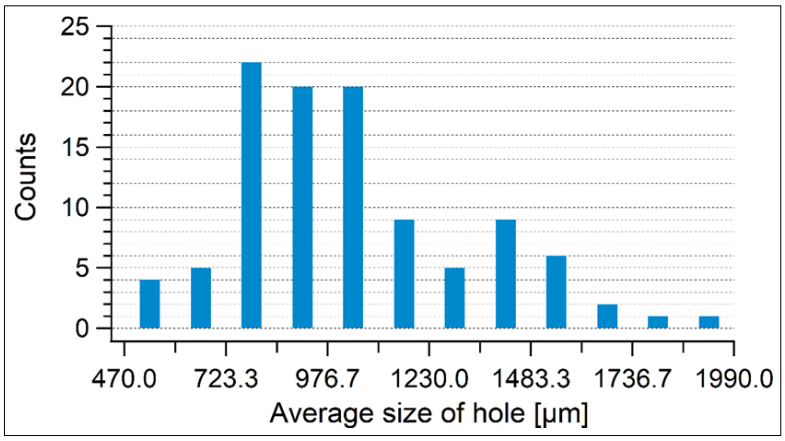

Fig. 3. Histogram for DLC/Cu samples with free-standing DLC film

The optical microscopy at 20X magnification (Fig. 4) on the Cu side of free-standing zones reveals that the substrate morphology (the striations) was transferred to the DLC film. The low traces of impurities stand out, having as possible sources the photoresist film, the incompletely corroded Cu material and the $FeCl_3$ solution bath. Nonetheless, they don't disturb the final purpose which involves only the conversion of DLC film to the plasma.

The HPL spot radius or waist, *w(z),* is given by Eq.(1), where z is the distance from the focus plane (i.e., the front surface of Al foil that is located at z=0), $z_0=\pi w_0^2/\lambda$, $w_0=2\lambda/\pi\Theta$, $\Theta=2cot^{-1}(2f/D)$, f and D are the focal length of the focusing mirror, and the diameter of the collimated beams, respectively [13]. The laser wavelength λ is ~810 nm and f/D is ~700 mm/190 mm for the set-up used in 1 PW ELI-NP experimental area [12].

$$w(z) = w_0\sqrt{1+\left(\frac{z}{z_0}\right)^2} \tag{1}$$

From Eq.(1), the HPL spot sizes on DLC were 5.57 µm, 8.95 µm, and 12.73 µm for spacers with thicknesses of 15 µm, 30 µm and 45 µm, respectively (Tab. 2).

Generally, the well-focused surface zones in the optical microscopy images from Fig. 4 are enough larger than the spot size of HPL pulse on DLC film. A range of 3.7 µm of focus level values with standard deviation (σ) of 1.1 µm were found within a previous test on microscope keeping the viewed point. Therefore, the thickness of the DLC-Al empty space is almost constant behind the flat regions of DLC surface ensuring nearly identical geometric conditions of interaction, considering σ.

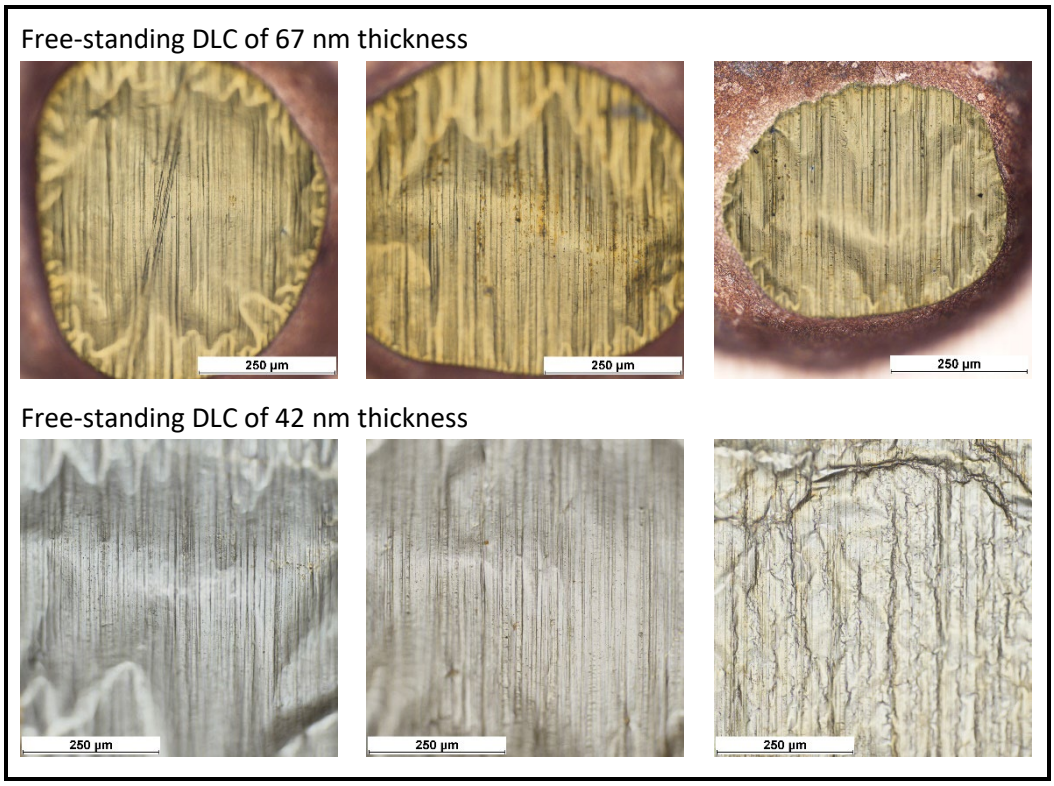

Fig. 4. Optical microscopy at 20X on free-standing DLC

The profilometry has provided the 3D profiles acquired on front surface of free-standing DLC films (scan area of ~175×132 µm^2). These data were processed in order to determine the surface roughness. From each representative 3D profile of 67 nm and 42 nm DLC thickness, three line profiles of ~100 µm length were extracted (Fig. 5, 6). These profiles were horizontally leveled by linear fit subtraction, such determining the 2D roughness (R_q) for each leveled profile z(x).

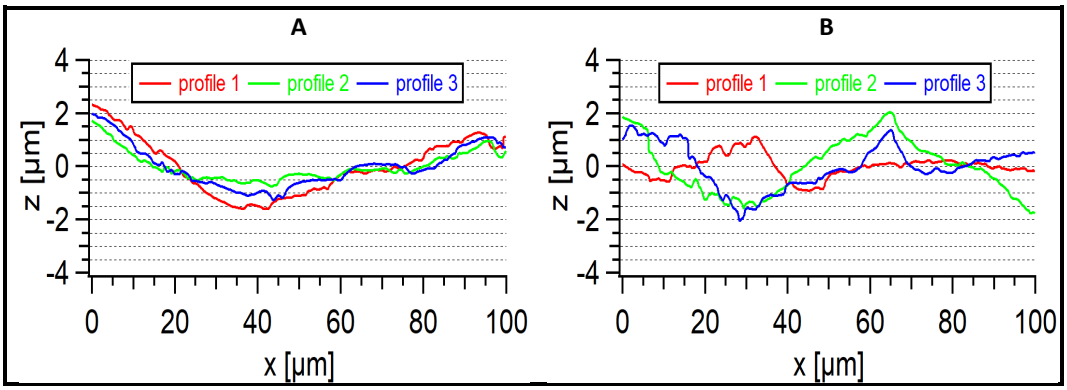

Fig. 5. Plots of leveled line profiles for DLC films of 67 nm (A) and 42 nm (B) thicknesses

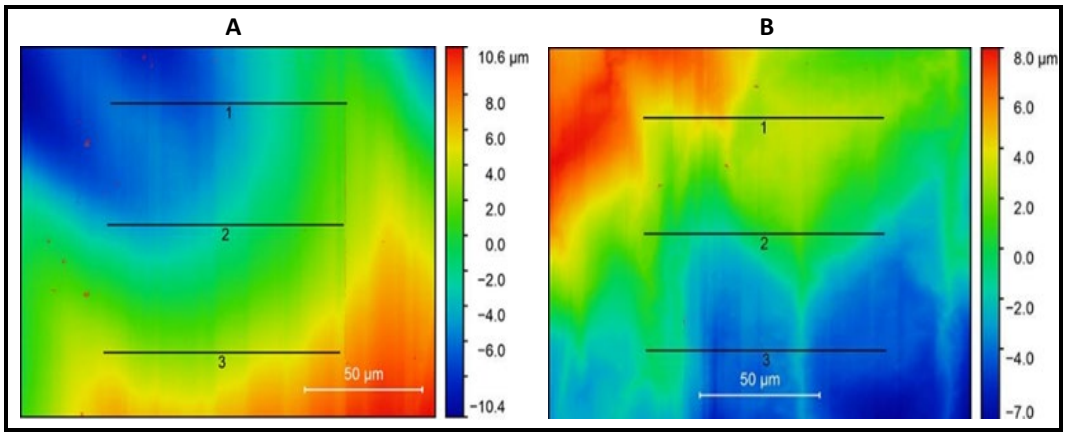

Fig. 6. The representative 3D profiles of DLC films of 67 nm (A) and 42 nm (B) thicknesses with the extracted line profile traces

The average roughness $R_{q\ average}$ is shown in Tab. 1 for each line profile and DLC thickness. The R_q values are ~15 times higher than DLC thicknesses, which strongly indicate a deviation from lamellar shape instead from thickness along profile traces. Therefore, the roughness is assimilated to the flatness in our case, whose value could not affect the properly functioning as explained in Section 4.

Table 1

Roughness of line profiles

Thickness [nm]	**(1)** Δz ; R_q [nm]	**(2)** Δz ; R_q [nm]	**(3)** Δz ; R_q [nm]	$R_{q\ average}$ [nm]
67	3923 ; 1051	2499 ; 539	3255 ; 780	3226 ; 790
42	2029 ; 429	3797 ; 1030	3578 ; 831	3135 ; 763

4. HPL experiment results

Four double targets were fabricated according to the design parameters from Tab. 2 and experimentally tested in HPL experiment for the occurrence of prepulse cleaning before incidence on an Al foil of 15 µm thickness. In the experiment, we have investigated the temporal contrast by evaluating the amplitude of the back-reflected pulses and the energy of the accelerated protons. The method used for this test was to compare the back-reflection between the double DLC-Al and single Al targets (Fig. 7, 8).

For a proper interaction and in the absence of prepulses, the main laser pulse would need to encounter a near solid density plasma. In the event of unwanted prepulses, generated from ns to tens of ps before the main pulse, interact with the front surface of the target a long scale preplasma may be generated affecting the main interaction and causing high amplitude back-reflected pulses.

Table 2

Construction parameters of double targets

Label	I	II	III	IV
DLC thickness [nm]	42	42	42	67
Spacer thickness [μm]	15	30	30	45

The double layer targets were shot with a peak laser intensity of ~10^{20} W/cm^2 during the commissioning phase of the 1 PW experimental area dedicated to laser-solid interaction. At this stage, several prepulses were measured in the -100 ps regime with several others in the ns regime. Fig. 7 shows the results obtained for the back-reflected (BR) pulses when using the double layer targets; while the results obtained with the sole Al target are shown in Fig. 8. It can be observed that the BR values are up to a factor 4 or higher for the double layer targets with respect to the Al foils.

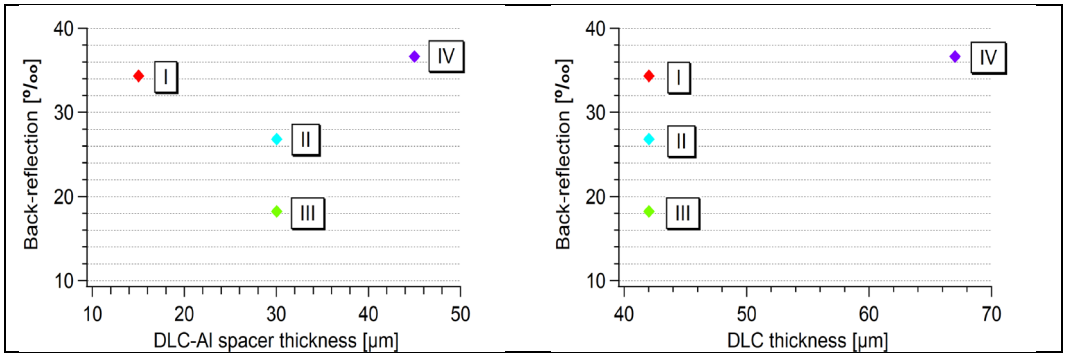

Fig. 7. Ratio of the back reflected light over the incident laser light for different double layer targets

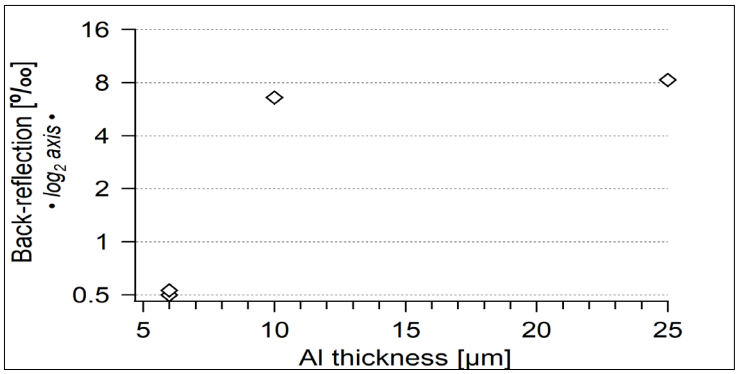

Fig. 8. Ratio of the back reflected light over the incident laser light for different Al foils of 4.5, 6, 10 and 25 μm thickness

These results can be explained by the presence of the multiple prepulses in the temporal structure (as indeed measured and removed later in further experiments) of the laser pulse that generate a long plasma layer in front of the main target. While the first prepulse would be absorbed in the thin DLC target, the other forthcoming prepulses can either be absorbed or transmitted through the expanded plasma then still affecting the main Al target. The interaction of multiple laser pulses starting from the ns down to ps scale with solid targets represents a complex subject of research that will not be treated here. 1D hydrodynamic simulations were performed in order to understand if more than one prepulse can lead to the observed effect. We considered two prepulses in the ns regime with peak intensity of 5×10^{13} W/cm^2 and pulse durations of 200 fs interacting with a 100 nm thick C target similarly to the experimental configuration. The first prepulse was interacting with the laser target at -20 ns, while the second at -1 ns prior to the main pulse. The plot of the electron density distribution over time shows that after the first prepulse interacts with the C layer the target starts to expand, and when the second pulse hits the target the electron plasma density rapidly expands as low as 10^{19} cm^{-3}. In this configuration, the ps regime prepulses first and the main pulse last will see and interact with a long scale preplasma that can affect the focusing depending on the prepulses position in time. Moreover, one can see that the expansion of the DLC plasma from the first prepulse interaction has a large spatial extent that travels 50 μm in ~7 ns. Therefore, after 7 ns the plasma plume will reach the second Al target, potentially also causing damage to it. The simulations show that the double layer target has limited effect in case of multiple prepulses.

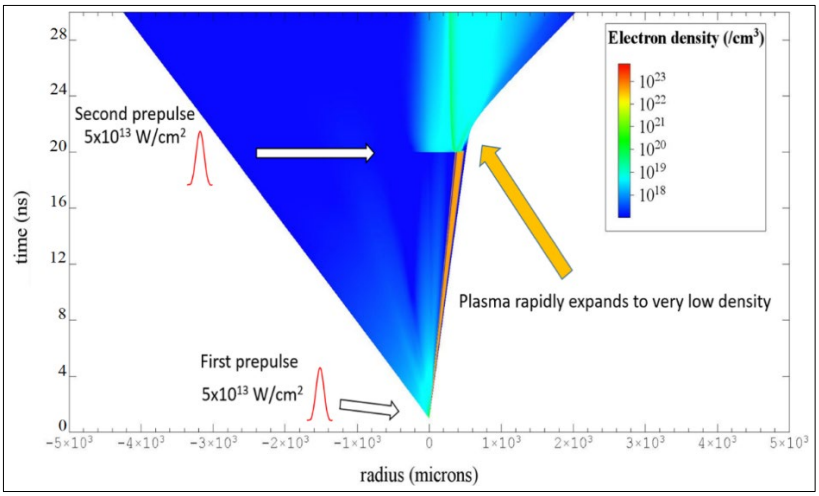

Fig. 9. 1D hydrodynamic simulation where 2 prepulses of intensity 5×10^{13} W/cm^2, 200 fs pulse duration spaced at 20 ns interacted with a 100 nm C target. The plasma expansion from the first prepulse reaches the second Al target after ~7 ns (not present in the simulation). The second prepulse is absorbed and rapidly expanding the remaining plasma to densities as low as 10^{19} cm^{-3}

The interaction dynamics of the main pulse with the plasma plume is also dependent on the 3D morphology of DLC thin film (e.g., flatness over regions comparable in size to the laser spot).

This is due to the plume velocity (~7×10^3 m/s in simulation), the plasma reaches a spatial extent of ~136 μm before the arrival of the second prepulse (after 19 ns) and even more until the main pulse, that is much more than σ (1.1 μm) and $R_{q\ average}$ (0.75÷0.80 μm) of the initial solid surface.

5. Conclusions

The proper functioning of the double-target ensembles involved in our experimental work is highly dependent on the temporal profile preceding the main pulse. A temporal profile consisting of a single prepulse of low intensity and in the ps regime would likely be absorbed by the DLC film helping with the back-reflection suppression. However, a single ns regime prepulse is capable of generating long plasma that can affect the main Al target foil. This situation can affect the interaction of the Al foil with the main laser pulse for example by altering the target surface and then bringing to an inappropriate interaction. The presence of multiple prepulses will have an even more complex interaction with the target bringing to additional effects. Hence, further research is needed to better understand the target requirements, as for instance the displacement between the DLC and the Al, even for a single prepulse to be successfully suppressed.

Acknowledgements

The fabrication and characterization have been made using the research infrastructure of The Targets Laboratory from ELI-NP and of The Plasma Processes, Materials and Surfaces Group from INFLPR. This research was supported by IFIN-HH from European and National Funds through POC project ELI-NP and Nucleus Program project no. PN 19 06 01 05 and PN 23 21 01 05, and by INFLPR. The Nucleus Program is funded by the Romanian Ministry of Research, Innovation and Digitalization.

R E F E R E N C E S

[1] *M. Pessot, P. Maine, G. Mourou,* 1000 times expansion/compression of optical pulses for chirped pulse amplification, Optics Communications 62, issue 6 (1987) 419-421. https://doi.org/10.1016/0030-4018(87)90011-3.

[2] *J. W. Yoon, C. Jeon, J. Shin, S. K. Lee, H. W. Lee, I. W. Choi, H. T. Kim, J. H. Sung, C. H. Nam,* Achieving the laser intensity of 5.5×10^{22} W/cm^2 with a wavefront-corrected multi-PW laser, Optics Express 27, issue 15 (2019) 20412-20420. https://doi.org/10.1364/OE.27.020412.

[3] *M. Roth, M. Schollmeier,* Ion Acceleration – Target Normal Sheath Acceleration, CERN Yellow Reports, Proceedings of The 2014 CAS-CERN Accelerator School: Plasma Wake Acceleration 1 (2016) 231. https://doi.org/10.5170/CERN-2016-001.231.

[4] *S. S. Bulanov, Q. Ji, S. Steinke, T. Schenkel, E. Esarey, W. P. Leemans,* Advanced Acceleration Mechanisms for Laser Driven Ions by PW-lasers, Proc. of 7th International Particle Accelerator Conference (IPAC 2016, Busan, Korea), JACoW (2016) 2082-2084. http://doi.org/10.18429/JACoW-IPAC2016-WEOAB01.

[5] *D. Sangwan, O. Culfa, C. P. Ridgers, S. Aogaki, D. Stutman, B. Diaconescu,* Simulations of carbon ion acceleration by 10 PW laser pulses on ELI-NP, Laser and Particle Beams 37 Issue 4 (2019) 346-353. https://doi.org/10.1017/S0263034619000648.

[6] *A. Magureanu, L. Dinca, C. Jalba, R. F. Andrei, I. Burducea, D. G. Ghita, V. Nastasa, M. Gugiu, T. Asavei, O. Budriga, D. Ticos, V. Craciun, B. Diaconescu, C. M. Ticos,* Target Characteristics Used in Laser-Plasma Acceleration of Protons Based on the TNSA Mechanism, Frontiers in Physics, Sec. Interdisciplinary Physics (2022) 10:727718. https://doi.org/10.3389/fphy.2022.727718.

[7] *L. A. Gizzi, E. Boella, L. Labate, F. Baffigi, P. J. Bilbao, F. Brandi, G. Cristoforetti, A. Fazzi, L. Fulgentini, D. Giove, P. Koester, D. Palla, P. Tomassini,* Influence of pre-plasma on accelerated protons in ultraintense laser interaction with not-so-thin foils, Research Square (2020) preprint version 1. https://doi.org/10.21203/rs.3.rs-68040/v1.

[8] *G. Doumy, F. Quere, O. Gobert, M. Perdrix, Ph. Martin, P. Audebert, J. C. Gauthier, J. P. Geindre, T. Wittmann,* Complete characterization of a plasma mirror for the production of high-contrast ultraintense laser pulses, Physical Review E 69 (2004) 026402. https://doi.org/10.1103/PhysRevE.69.026402.

[9] *M. Cernaianu,* Laser produced plasma optics, ELI Summer School 2019 - 'Nuclear Physics with High Power Lasers'. https://indico.eli-np.ro/event/72/timetable/#20190910.

[10] *M. Passoni, A. Zani, A. Sgattoni, D. Dellasega, A. Macchi, I. Prencipe, V. Floquet, P. Martin, T. V. Liseykina, T. Ceccotti,* Energetic ions at moderate laser intensities using foam-based multi-layered targets, Plasma Physics and Controlled Fusion 56 (2014) 045001. https://dx.doi.org/10.1088/0741-3335/56/4/045001.

[11] *M. Passoni, A. Sgattoni, I. Prencipe, L. Fedeli, D. Dellasega, L. Cialfi, I. W. Choi, I J. Kim, K. A. Janulewicz, H. W. Lee, J. H. Sung, S. K. Lee, C. H. Nam,* Toward high-energy laser-driven ion beams: Nanostructured double-layer targets, Physical Review Accelerators and Beams 19 (2016) 061301. https://doi.org/10.1103/PhysRevAccelBeams.19.061301.

[12] *M. O. Cernăianu, P. V. Ghenuche, et al.,* Commissioning of the 1 PW experimental area with an experiment on TNSA ion acceleration, ELI-NP Annual Report 2020-2021 (2022) 91-93. https://www.eli-np.ro/documents/ELI-NP-Annual_Report-2020-2021.pdf.

[13] *M. Divall,* Beam Shaping, First International School on laser Applications - LA³NET (2012) LA³NET Consortium. https://indico.cern.ch/event/177701/contributions/1441170.